THE MINERALOGIC IMPLICATIONS OF IMPACT-INDUCED CLIMATE PERTURBATIONS: INSIGHT FROM CONDUCTION AND REACTIVE TRANSPORT MODELING. S. V. Kaufman[1], A. M. Palumbo[1], E. Bjonnes[2], J. F. Mustard[1], [1]Brown University, Department of Earth, Environmental, and Planetary Sciences, Providence, RI, [2]Lunar and Planetary Institute, Houston, TX (sierra_kaufman@brown.edu)

Introduction: Robust 3D climate modeling of Mars has led to the framework of a cold and icy background climate that is unable to maintain temperatures high enough to support sustained liquid water [1–3]. Due to the abundant geomorphic [4–6] and mineralogic [7–10] evidence for liquid water on the martian surface, work has been ongoing to test hypotheses regarding punctuated heating events that could bring above-freezing temperatures in an otherwise cold climate in the Late Noachian and Early Hesperian [11–19].

The timescales and magnitudes of these punctuated heating events have implications for what features can be formed by the surface water that results from increased temperatures and melting of surface ice or rainfall; understanding the required timescales to form the observed geomorphic and mineralogic properties provide insight into the necessary duration of these punctuated heating events. Previous studies have assumed approximate terrestrial temperatures and rainfall rates to determine the amount of time to produce the observed geomorphic and mineralogic features. The largest valley networks, for example, may have taken as little as 200-5000 years to form [20] and therefore require heating to have lasted for at least that long. Previous work has shown that hydrous mineralogy may develop during multiple climate perturbations; however, each perturbation would be required to have lasted tens of thousands of years and have occurred multiple times [21]. Therefore, much longer timescales are necessary to explain the mineralogic signatures than geomorphic features.

Heating due to impact events creates significantly more extreme environments than other heating mechanisms. Impact cratering has been shown to create rainfall at boiling temperature and higher rain rate (2.6 m/yr.) than rainforests on Earth [17]. A basin-forming impact cratering event may deposit a global silicate layer [12,13], extending the duration of the intense rainfall [14]. As water vapor condenses out of the atmosphere and hits this global, hot silicate layer, it re-vaporizes, causing a transient water cycle which persists until the entirety of the silicate layer cools below the boiling point [14,16]. These extended high rain rates at extremely high temperatures may have caused clay formation on early Mars [16]. If possible, this method of clay formation would operate over significantly less time than the previously hypothesized episodes of tens of thousands of years.

This work determines the expected mineralogic assemblage from the climate perturbations following a basin-scale impact event to determine if it is a viable hypothesis for forming clay minerals. We do this through conduction modeling followed by reactive transport modeling.

Methods: We build upon previous work which calculated the extent of time needed to cool a global silicate layer initially deposited at 1600 K [14]. The original calculations for the length of time the silicate layer would extend the induced climate effects was a simple energy calculation [14]:

$$Rain\ duration\ (yrs) = \frac{thermal\ energy\ in\ layer\ (J)}{energy\ removed\ by\ global\ \ rainfall\ (J/yr)}$$

For an Argyre sized impact, this would result in just over 200 years of additional rain [14]. Here, we introduce a more quantitatively detailed approach to revise this estimate of extended rain duration or, in other words, the amount of time to cool the silicate layer via rainfall: we consider the effects of conduction downward into the crust, the temperature variable heat capacity, and partial melting of the silicate layer.

Conduction Modeling. We developed a 1D finite-difference heat conduction model with a 34 m thick silicate layer (consistent with an Argyre-sized impact) starting at 1600 K overlying a cold (273 K) crust. Our model uses an arbitrarily thick crust to minimize boundary effects from holding the temperature at the base of the crust constant at 273 K.

Our model simulates cooling of an emplaced silicate layer as follows, where initially, the entire silicate column is 1600 K. We assume a constant-rate deposition of water and run the model at 1-hour timesteps, which is sufficient to capture the desired trends. We introduce a heat flux boundary condition in order to simulate the behavior of water percolating through the layer until it hits material above its boiling point and evaporated: the shallowest cell (each cell is 1 m thick) above 373 loses a consistent amount of heat based on a rain rate of 2.6 m/yr [17]. This boundary condition starts at the top cell, but when it drops below the boiling point of water, the heat loss then comes from the shallowest cell above 373 K and the top cell is then set to either its temperature in the previous timestep or that of the cell below it, whichever is lower.

Temperature-Dependent Heat Capacity. Mars has a basaltic crust that does not show evidence of significant processing [22]. Stony meteorites are predicted to be more common in the inner Solar System [23,24] but the volume of projectile material is not sufficient to have an effect on the overall composition of the emplaced silicate layer. We therefore assume a basaltic composition for the emplaced silicate layer and underlying crust. The temperature-dependent heat capacity of basalt is described by the equation below [25]:

$$C_p\left(\frac{cal}{g * ºC}\right) = 0.2356 + 4.3635 * 10^{-5}T - \frac{6.3440 * 10^3}{T^2}$$

Due to the wide temperature range experienced during the cooling of the silicate layer, the temperature dependence of the heat capacity can make a significant difference in cooling time. Although we remove the same amount of energy from the silicate layer in each timestep through the evaporation of the rain, the amount of temperature change varies because of heat capacity variation.

Phase Transition of Basalt. The liquidus of basalt is between 1448-1623 K [26]. Therefore, the silicate layer will be partially molten upon deposition to the surface and will solidify as the layer cools. We assume a linear relationship between the melt fraction and the melting temperature for simplicity.

Reactive Transport Modeling. The conduction model outputs a temperature profile of the silicate layer and underlying crust as a function of time. To determine the mineralogic implications of the impact-induced climate perturbations, we will use this output and the rainfall rates previously calculated [17] with the reactive transport model CrunchFlow [27,28].

We will use permeability and porosity values consistent with a welded tuff [29] and a protolith of basaltic glass [30] for the silicate layer. Alteration time and temperature will be taken from the results of the conduction model, and incoming water is pH-neutral with no dissolved load.

Preliminary Results: We have completed preliminary runs of our conduction model. The phase transition is currently in the implementation stage as a part of the conduction model code; the results reported here do not account for these effects and treat the whole layer as a solid. Our conduction model with a constant

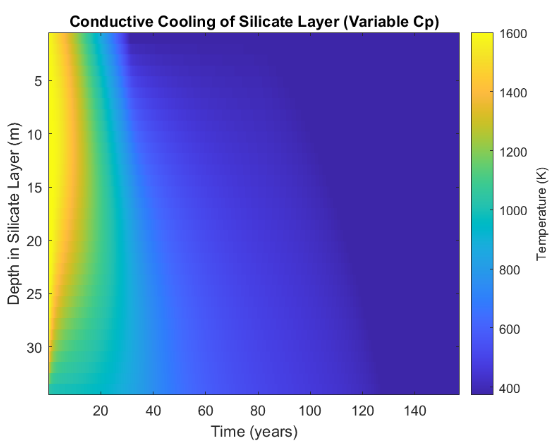

***Figure 1**. Conductive cooling of silicate layer using a variable heat capacity for basalt [25]. Color represents the average temperature in a cell at a given time.*

heat capacity of basalt results in cooling of the entire silicate layer to below the boiling point of water in 114 years.

When accounting for the temperature-dependence, the heat capacity of basalt increases with temperature, decreasing thermal diffusivity and slowing the heat transfer. This causes the layer to take 157 years to cool (Figure 1). This timescale is notably less than the original >200 years reported by [14] mainly due to the effects of conduction downward into the crust.

Conclusions: The modified model presented here includes the more realistic temperature-dependent heat capacity for an emplaced layer of basalt, and reduces the expected lifetime of impact-induced climate effects. Future work will include the phase transition of basalt and introduce these temperature profiles and assumed rainfall rates into CrunchFlow to determine the mineralogic implications of impact-induced climate perturbations.

These revised estimates of rainfall durations and mineralogic alteration due to impact-induced climate perturbations will be critical to constraining the climate history: if the observed surface mineralogic alteration is explained with these relatively short-term periods of punctuated heating, there may be no need for thousands of years of warm temperatures and rainfalls as has been previously assumed.

References: [1] Wordsworth, R. et al. (2013) *Icarus*, *222*, 1–19. [2] Wordsworth, R. et al. (2015) *JGR: Planets*, *120*, 1201–1219. [3] Forget, F. et al. (2013) *Icarus*, *222*, 81–99. [4] Fassett, C. I. and Head, J. W. (2008) *Icarus*, *195*, 61–89. [5] Irwin, R. P. et al. *River Confluences, Tributaries and the Fluvial Network*, (2008), p. 419. [6] Fassett, C. I. and Head, J. W. (2005) *GRL*, *32*. [7] Poulet, F. et al. (2005) *Nature*, *438*, 623–627. [8] Bibring, J.-P. et al. (2006) *Science*, *312*, 400–404. [9] Mustard, J. F. et al. (2008) *Nature*, *454*, 305–309. [10] Ehlmann, B. L. et al. (2009) *JGR*, *114*. [11] Halevy, I. and Head III, J. W. (2014) *Nat. Geosci*, *7*, 865–868. [12] Segura, T. L. et al. (2002) *Science*, *298*, 1977–1980. [13] Segura, T. L. et al. (2008) *JGR*, *113*. [14] Toon, O. B. et al. (2010) *Annu. Rev. Earth Planet Sci.*, *38*, 303–322. [15] Segura, T. L. et al. (2012) *Icarus*, *220*, 144–148. [16] Palumbo, A. M. and Head, J. W. (2018) *MAPS*, *53*, 687–725. [17] Turbet, M. et al. (2020) *Icarus*, *335*, 113419. [18] Palumbo, A. M. et al. (2018) *Icarus*, *300*, 261–286. [19] Mischna, M. A. et al. (2013) *JGR: Planets*, *118*, 560–576. [20] Hoke, M. R. T. et al. (2011) *EPSL*, *312*, 1–12. [21] Bishop, J. L. et al. (2018) *Nat. Astron*, *2*, 206–213. [22] Wyatt, M. B. and McSween, H. Y. (2002) *Nature*, *417*, 263–266. [23] Davison, T. M. et al. (2010) *Icarus*, *208*, 468–481. [24] Davison, T. M. et al. (2012) *Geochim. Cosmochim. Acta*, *95*, 252–269. [25] Peck, D. L. *Cooling and Vesiculation of Alae Lava Lake, Hawaii*, (1978). [26] Dzhigiris, D. D. et al. (1983) *Glass Ceram*, *40*, 467–470. [27] Steefel, C. I. and Lasaga, A. C. (1994) *Am J Sci*, *294*, 529–592. [28] Steefel, C. I. and MacQuarrie, K. T. B. *Reactive Transport in Porous Media*, (1996). [29] Reda, D. C. and Hadley, G. R. (1986) *Environ. Geol. Water Sci*, *8*, 137–145. [30] Simonson, B. M. and Glass, B. P. (2004) *Annu. Rev. Earth Planet Sci.*, *32*, 329–361.